On the condensed history technique for electron transport

I. Kawrakow [a,*], Alex F. Bielajew [a,b]

[a] *Inst. for Nat. Measurement Standards, Ionizing Radiation Standards, National Research Council of Canada, Ottawa, Ont., Canada K1A 0R6*

[b] *Department of Nuclear Engineering and Radiological Sciences, The University of Michigan, Cooley Building, 2355 Bonisteel Boulevard, Ann Arbor, MI, USA*

Received 10 February 1998

Abstract

In this report we discuss the theory of the "condensed history technique", an approximate solution to the Boltzmann transport equation that sums the effect of up to thousands of discrete, small momentum transfer elastic and inelastic collisions into single larger-effect quasi-events. This technique saves much calculational effort at the expense of introducing errors that are now understood quantitatively in terms of the development presented herein. We apply our analysis to modern realizations of the condensed history method, namely those of EGS/PRESTA, ETRAN/TLC, FLUKA, PENELOPE, and LLCA. We have also constructed an algorithm that exhibits smaller large step size instabilities than all of these methods and give several examples. © 1998 National Research Council of Canada, Published by Elsevier Science B.V.

1. Introduction

The transport problem of particles in matter can be solved exactly, within the existing knowledge of the elementary collision processes, by the analog [1] Monte Carlo technique. Monte Carlo simulations of particle transport processes are a faithful simulation of physical reality: particles are "born" according to distributions describing the source, they travel a certain distance (determined by a probability distribution) to the site of a collision and scatter into another energy and/or direction. This procedure is continued until the particle is absorbed or leaves the geometry under consideration. Quantities of interest can be calculated by averaging over a given set Monte Carlo particle "histories". The statistical uncertainty of the calculation depends on N, the number of particle histories simulated, and decreases as $N^{-1/2}$. Depending on the desired accuracy or the complexity and size of the geometry, this may lead to very long calculation times.

---

[*] Corresponding author. Tel.: 613 993 2197; fax: 613 952 9865; e-mail: iwan@irs.phy.nrc.ca.
[1] By "analog" Monte Carlo we mean true event-by-event Monte Carlo without any variance reduction or physics input other than cross sections.

An additional difficulty occurs in the case of the simulation of electron transport. In the process of slowing down, a typical fast electron undergoes of the order of 10^5–10^6 collisions with surrounding matter. Because of this large number of interactions, an analog simulation of electron transport is often not practical. To circumvent this difficulty, Berger [1] developed the "condensed history" technique. In this method, large numbers of transport and collision processes are "condensed" to a single electron step. The cumulative effect of the individual interactions is taken into account by the appropriate change of the particle's energy and direction of motion at the end of the step. This approach was motivated by the fact that single collisions with the atoms cause in most cases only minor changes in the particle's energy and direction of flight.

Recently, Larsen [2] has provided a mathematical proof that the condensed history technique is a solution to the Boltzmann transport equation in the limit of small step size. He has shown that conventional realizations of the method have an $O(\Delta s)$ truncation error, where Δs is the path-length of the step, proposed an $O(\Delta s^2)$ version of the method and indicated that higher-order solutions may possibly be devised by splitting the operations of transport and scattering along a transport step.

In this article we analyze different realizations of the condensed history technique in terms of a direct comparison with the moments of the spatial distributions and spatial-angular correlations. Our analysis seems to indicate that the order of the truncation error cannot be reduced by simply "mixing" different operator-split procedures. Finally, we propose a new electron transport algorithm which has a higher order truncation error than previously proposed algorithms, at least for the low-order spatial moments and spatial-angular correlations that we have investigated.

The remaining part of the paper is organized as follows. In Section 2 we summarize basic formulae and notation used throughout the paper. In Section 3, existing electron transport algorithms are analyzed. In Section 4 possible new algorithms are discussed. A simple example is presented in Section 5. The results are discussed and summarized in Section 6.

2. Some basic formulas and notation

We consider the transport of electrons in a condensed history Class II scheme [1]. That is to say, the bremsstrahlung process that results in the creation of photons above an energy threshold E_γ, and Møller knock-on electrons set in motion above an energy threshold E_δ, are treated discretely by creation and transport. Sub-threshold processes are accounted for in a continuous slowing down approximation (CSDA) model. For further description of the Class II scheme the reader is encouraged to read Berger's article [1] who coined the terminology and gave a full description and motivation for the classification scheme.

If the direction of motion is given by the unit vector $\vec{v}$, the position by $\vec{x}$, the cross section for elastic scattering per unit solid angle by σ and if energy loss is taken into account by considering the energy as a function of the residual range of the particles, the electron transport process between interaction vertices is governed by the following transport equation

$$\frac{\partial f(s; \vec{x}, \vec{v})}{\partial s} + \vec{v}\vec{\nabla}f(s; \vec{x}, \vec{v}) = N \int d\vec{v'}\left[f(s; \vec{x}, \vec{v'}) - f(s; \vec{x}, \vec{v})\right]\sigma(\vec{v}\cdot\vec{v'}). \qquad (1)$$

Here, s is the arc length traversed by the particle and N is the number of atoms per unit volume. Lewis [3] provided a formal solution of the above equation in terms of the longitudinal and transverse moments of the phase space distribution function $f(x, y, z, \cos\theta, \phi)$. A generalization of Lewis' method which allows the calculation of arbitrary moments $\langle x^{n_x} y^{n_y} z^{n_z} v_x^{m_y} v_y^{m_y} v_z^{m_z} \rangle$ is given in Appendix A.

In this article we will discuss different Monte Carlo electron transport algorithms and compare the resulting moments to the exact one's derived by Lewis. We will consider up to second order moments, i.e. $\langle z \rangle, \langle zv_z \rangle, \langle z^2 \rangle, \langle xv_x + yv_y \rangle$ and $\langle x^2 + y^2 \rangle$. Assuming that the initial position is at the origin and the initial direction along the z-axis, Lewis' method gives:

$$\langle z \rangle = \int_0^s ds' k_1(s'),$$

$$\langle z v_z \rangle = \frac{1}{3} \int_0^s ds' k_1(s - s') [1 + 2k_2(s')],$$

$$\langle x v_x + y v_y \rangle = \frac{2}{3} \int_0^s ds' k_1(s - s') [1 - k_2(s')],$$

$$\langle z^2 \rangle = \frac{2}{3} \int_0^s ds' \int_0^{s'} ds'' k_1(s' - s'') [1 + 2k_2(s'')],$$

$$\langle x^2 + y^2 \rangle = \frac{4}{3} \int_0^s ds' \int_0^{s'} ds'' k_1(s' - s'') [1 - k_2(s'')]. \tag{2}$$

Here, k_i is short hand notation for

$$k_i(s) = \exp \left[- \int_0^s ds' \kappa_i(s') \right], \tag{3}$$

where the κ's are the moments of the single scattering cross section $\sigma(\chi)$,

$$\kappa_i(s) = 2\pi N \int_{-1}^1 d \cos \chi \sigma(\chi, s') [1 - P_i(\cos \chi)]. \tag{4}$$

In the above equation P_i denote the Legendre polynomials. In the following discussion we will frequently use the first two multiple scattering moments and give them therefore their own notation:

$$\xi = \int_0^s ds' \kappa_1(s'),$$

$$\gamma = \frac{\kappa_2}{\kappa_1}. \tag{5}$$

At very high energies where the single scattering cross section is strongly forward peaked, γ approaches 3. At very low energies, where the single scattering cross section is almost isotropic, γ goes to unity. For energies above few keV, γ is always bigger then two and, for a given material, a very slowly varying function of energy.

We will also need the average cosine and sine squared of the multiple scattering angle. From the theory of Goudsmit and Saunderson [4,5] we have

$$f(s; \cos \theta) = \int d\phi \int dx \, dy \, dz \, f(s; x, y, z, \cos \theta, \phi) = \sum_{i=0}^{\infty} \left(i + \frac{1}{2} \right) k_i(s) P_i(\cos \theta), \tag{6}$$

and therefore:

$$\langle \cos \theta \rangle = k_1(s),$$

$$\langle \sin^2\theta \rangle = \frac{2}{3}[1 - k_2(s)]. \tag{7}$$

To simplify the following analysis we will neglect energy loss. Then we have

$$\xi = \sigma_T s \approx \frac{T_s s}{2} \tag{8}$$

where σ_T is the transport cross section [6] and T_s the linear scattering power [7]. The approximate equation holds for small-angle scattering. In addition, to be able to demonstrate the deviations from the exact answer resulting from the different transport algorithms, we will frequently expand the various expressions in a power series in ξ. For instance, we obtain from Eq. (2):

$$\frac{s - \langle z \rangle}{s} = \frac{\xi}{2}\left(1 - \frac{\xi}{3} \pm \cdots\right),$$

$$\frac{\langle zv_z \rangle - \langle z \rangle \langle v_z \rangle}{s} = \xi\left(\frac{3 - \gamma}{3} + \frac{\gamma^2 + \gamma - 9}{9}\xi \pm \cdots\right),$$

$$\frac{\langle xv_x + yv_y \rangle}{s} = \xi\left(\frac{\gamma}{3} - \frac{\gamma(\gamma + 1)}{9}\xi \pm \cdots\right),$$

$$\frac{\langle z^2 \rangle - \langle z \rangle^2}{s^2} = \xi\left(\frac{2(3 - \gamma)}{9} + \frac{\gamma^2 + \gamma - 9}{18}\xi \pm \cdots\right),$$

$$\frac{\langle x^2 + y^2 \rangle}{s^2} = \xi\left(\frac{2\gamma}{9} - \frac{\gamma(\gamma + 1)}{18}\xi \pm \cdots\right). \tag{9}$$

The first equation expresses the difference between the curved electron path-length and the transport along the initial direction of motion and has become known as "path-length-correction" or the "detour" correction. The second and third equations give the correlation strength between the final position and final direction of motion. If the final position was independent of the final direction of motion these correlations would be zero. The last two equations describe the straggling of the electron position around the mean value. It is apparent from Eq. (9) that the error introduced by a simple condensed history algorithm, where particles are transported along the initial direction of motion, will become negligible for sufficiently small step sizes ($\xi \to 0$). This observation is in agreement with Larsen's operator formalism proof [2]. It is also clear that detours due to multiple scattering are better described in terms of ξ instead of the path-length (or the fraction of the residual range of the particles). We will therefore use ξ as a measure of step lengths in the remaining part of the paper.

If the exact solution of Eq. (1), $f(s; \vec{x}, \vec{v})$, were known, particle transport between discrete interaction vertices could be done in a single step. As this solution is not known yet, other step size restrictions have to be applied. One popular choice is a constant fractional energy loss per step, ϵ, built into the ETRAN Monte Carlo code [1,8,9], and introduced by Rogers [10] into EGS4 [11]. The empirical observation that a smaller ϵ has to be used in high Z materials in order to obtain correct results [12,13] is readily understood in terms of Eq. (9) and Fig. 1, where ξ is plotted as a function of kinetic energy E for three different materials and $\epsilon = 0.1$. As ξ is proportional to ϵ,

$$\xi = \sigma_T s = \frac{\sigma_T E}{L(E, E_\gamma, E_\delta)}\epsilon, \tag{10}$$

ξ-values for other fractional energy losses can be obtained by multiplication with the appropriate factor. Here, $L(E, E_\gamma, E_\delta)$ denotes the restricted stopping power for threshold energies of E_γ and E_δ (see the begin-
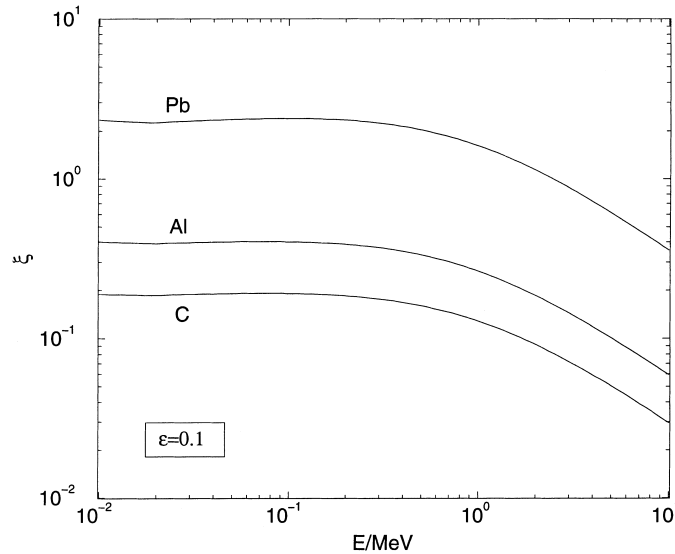
Fig. 1. The transport parameter ξ (see Eqs. (4), (5), (8) and (10)) for a path-length corresponding to 10% energy loss as a function of kinetic energy for different materials.

ning of this section). The transport cross section has been calculated for simplicity from a screened Rutherford cross section with a screening parameter as derived by Molière [14]. This is not particularly a good approximation for the single scattering cross section, yet it gives a reasonable first estimate of the scattering power of a medium [6]. It is not our intention to present an exact description of ξ as a function of ϵ here but rather to give the reader a better understanding of the deviations from the exact answer caused by the various transport algorithms discussed in Section 3.

3. Analysis of present algorithms

In this section we will discuss several existing electron transport algorithms and compare the resulting moments to the exact one. To simplify the analysis we will not consider the differences resulting from the different multiple scattering theories used, but will assume that all multiple scattering theories yield the correct result for $\langle \cos \theta \rangle$ and $\langle \sin^2\theta \rangle$.

3.1. Simple

In a simple condensed history algorithm, where particles are transported along the initial direction of motion and lateral deflections are neglected, the relative error will be $O(\xi^0)$. We have, for instance,

$$\frac{\langle xv_x + yv_y \rangle_{\text{simple}} - \langle xv_x + yv_y \rangle}{\langle xv_x + yv_y \rangle} = -1. \tag{11}$$

A simple algorithm is presently implemented in EGS4 (without PRESTA [11], in the ITS system [17] and in the electron component of MCNP [18,19]).

3.2. PRESTA

According to PRESTA [15,16], an electron transport option of EGS4 [11], at the end of the step the electron is transported along the initial direction of motion to $\langle z \rangle$, whereas the lateral displacement is related to the final scattering angle, i.e:

$$z = \langle z \rangle,$$

$$x = \frac{s}{2} \sin \theta \cos \phi,$$

$$y = \frac{s}{2} \sin \theta \sin \phi. \tag{12}$$

This procedure will give the exact result for $\langle z \rangle$ (provided the exact result for $\langle z \rangle$ is used) but under-estimates the second longitudinal moment

$$\frac{\langle z^2 \rangle_{\mathrm{PRESTA}} - \langle z^2 \rangle}{\langle z^2 \rangle} = \frac{\langle z \rangle^2}{\langle z^2 \rangle} - 1 \approx -\frac{2(3 - \gamma)}{9} \xi - \frac{\gamma^2 + 21\gamma - 45}{162} \xi^2 \pm \cdots \tag{13}$$

The correlation between z and v_z is also under-estimated

$$\frac{\langle z v_z \rangle_{\mathrm{PRESTA}} - \langle z v_z \rangle}{\langle z v_z \rangle} = \frac{\langle z \rangle \langle \cos \theta \rangle}{\langle z v_z \rangle} - 1 \approx -\frac{3 - \gamma}{3} \xi - \frac{5\gamma - 9}{18} \xi^2 \pm \cdots \tag{14}$$

The correlation between the transverse position and direction of motion, $\langle x v_x + y v_y \rangle$, is under-estimated at high energies (where $\gamma > 2$) and over-predicted at very low energies:

$$\frac{\langle x v_x + y v_y \rangle_{\mathrm{PRESTA}} - \langle x v_x + y v_y \rangle}{\langle x v_x + y v_y \rangle} = \frac{s \langle \sin^2 \theta \rangle}{2 \langle x v_x + y v_y \rangle} - 1 \approx -\frac{\gamma - 2}{6} \xi + \frac{\gamma^2 - \gamma + 1}{36} \xi^2 \pm \cdots \tag{15}$$

Finally, we obtain for the second order transverse moment

$$\frac{\langle x^2 + y^2 \rangle_{\mathrm{PRESTA}} - \langle x^2 + y^2 \rangle}{\langle x^2 + y^2 \rangle} = \frac{s^2 \langle \sin^2 \theta \rangle}{4 \langle x^2 + y^2 \rangle} - 1 \approx -\frac{1}{4} + \frac{3(\gamma - 1)}{16} \xi + \frac{13\gamma^2 - 12\gamma + 3}{320} \xi^2 \pm \cdots \tag{16}$$

i.e. it is under-estimated even for very short step sizes.

The derivations for $\langle x v_x + y v_y \rangle$ and $\langle x^2 + y^2 \rangle$ ignore the fact that in PRESTA the transport distance perpendicularly to the initial direction of motion must be reduced in some cases to guarantee that $x^2 + y^2 + z^2 \leqslant s^2$. This implies the condition

$$\sin^2 \theta \leqslant 4 \left(1 - \frac{\langle z \rangle^2}{s^2} \right) \approx \xi \left(1 - \frac{7}{12} \xi \pm \cdots \right). \tag{17}$$

The right-hand side of Eq. (17) is smaller than unity for $\xi \leqslant 0.295$ and so electrons will be placed at $r^2 = s^2 - \langle z \rangle^2$ every time a multiple scattering angle not satisfying Eq. (17) is sampled leading to a reduction of $\langle x v_x + y v_y \rangle$ and $\langle x^2 + y^2 \rangle$ (for a more detailed discussion of this issue see Ref. [25]). An analytical calculation for $\langle x v_x + y v_y \rangle$ and $\langle x^2 + y^2 \rangle$ is not possible in this case and we have therefore used Eqs. (15) and (16) to calculate PRESTA results shown in Figs. 4 and 6 (see Section 3.7).

The overall relative error of the algorithm is $O(\xi^0)$.

3.3. ETRAN/TLC

In his pioneering work on electron transport Monte Carlo, Berger [1] proposed to use the following simple relation between final scattering angle and final co-ordinates [2]:

$$x = \frac{s}{2}(\sin\theta\cos\phi + \delta_x),$$
$$y = \frac{s}{2}(\sin\theta\sin\phi + \delta_y),$$
$$z = \frac{s}{2}(1 + \cos\theta), \tag{18}$$

where δ_x and δ_y are random numbers that are distributed independently according to a Gaussian distribution with mean zero and variance $\sqrt{\langle\theta^2\rangle/6}$. When sampling on the basis of these formulas, one must of course exclude very large values of δ_x and δ_y for which $x^2 + y^2 + z^2 > s^2$. Berger argued that this should be extremely unlikely. We found however, that for typical step sizes currently in use in EGS4, this situation occurs in 20–30% of all cases. We get for the first order moments from Eq. (18):

$$\frac{\langle z\rangle_{\text{ETRAN}} - \langle z\rangle}{\langle z\rangle} = \frac{s(1 + \langle\cos\theta\rangle)}{2\langle z\rangle} - 1 \approx \frac{\xi^2}{12} \pm \cdots,$$

$$\frac{\langle zv_z\rangle_{\text{ETRAN}} - \langle zv_z\rangle}{\langle zv_z\rangle} = \frac{s(\langle\cos\theta\rangle + \langle\cos^2\theta\rangle)}{2\langle zv_z\rangle} - 1 \approx \frac{2\gamma^2 - 4\gamma + 3}{36}\xi^2 \pm \cdots,$$

$$\frac{\langle xv_x + yv_y\rangle_{\text{ETRAN}} - \langle xv_x + yv_y\rangle}{\langle xv_x + yv_y\rangle} = \frac{s\langle\sin^2\theta\rangle}{2\langle xv_x + yv_y\rangle} - 1 \approx -\frac{\gamma - 2}{6}\xi + \frac{\gamma^2 - \gamma + 1}{36}\xi^2 \pm \cdots, \tag{19}$$

i.e. they are all correct to $O(\xi)$ or better. For the second order longitudinal moment we have

$$\frac{\langle z^2\rangle_{\text{ETRAN}} - \langle z^2\rangle}{\langle z^2\rangle} = \frac{s^2(1 + 2\langle\cos\theta\rangle + \langle\cos^2\theta\rangle)}{4\langle z^2\rangle} - 1 \approx -\frac{3 - \gamma}{18}\xi + \frac{13\gamma^2 - 24\gamma + 36}{324}\xi^2 \pm \cdots \tag{20}$$

In order to reproduce the second order longitudinal moment,

$$\frac{\langle\delta_x^2 + \delta_y^2\rangle}{\langle x^2 + y^2\rangle} = 1 - \frac{s^2\langle\sin^2\theta\rangle}{4\langle x^2 + y^2\rangle} \approx \frac{1}{4} + \frac{3(\gamma - 1)}{16}\xi - \frac{3 - 12\gamma + 13\gamma^2}{320}\xi^2 \pm \cdots \tag{21}$$

has to be used for the δ's. With this the accuracy of Berger's algorithm for the moments studied here will be $O(\xi)$, i.e. an order of magnitude better than PRESTA.

3.4. FLUKA

Ferrari et al. [20] proposed and implemented in FLUKA [21] the following transport algorithm (we use here their notation):

---

[2] When energy loss is disregarded, Berger's algorithm is equivalent to the algorithm proposed by Larsen [2]. It should also be noted that most of Berger's algorithm was not included in ETRAN until Seltzer [9] introduced the TLC version of ETRAN. Before then, ETRAN (and also its well-known progeny, the ITS system [17] and the electron component of MCNP [18,19]) ignored lateral correlation and detour corrections, i.e. total path-length s and forward drift z were equated.

$$z = p \cos \eta,$$
$$x = p \sin \eta \cos (\phi + \Delta \omega),$$
$$y = p \sin \eta \sin (\phi + \Delta \omega),$$
$$p = p_{\text{corr}}(\cos \theta \cos \eta + \sin \theta \sin \eta \cos \Delta \omega) + p_{\text{uncorr}},$$
$$\eta = \rho \theta, \quad \cos \Delta \omega = \frac{1}{2\rho}. \tag{22}$$

Molière's theory [14,22] and approximate expressions for $\langle z \rangle, \langle z^2 \rangle$ were then used to calculate the free parameters $p_{\text{corr}}, p_{\text{uncorr}}$ and ρ. Because their approach is a priori based on the small-angle approximation, we will also use the small-angle approximation to analyze this algorithm. To do so, we expand the expressions for the various moments in a power series of θ^2 up to $O(\theta^4)$ and use

$$\langle \theta^2 \rangle \approx \frac{2(12 - \gamma)}{9} \xi - \frac{12 - \gamma^2}{9} \xi^2 \pm \cdots ,$$
$$\langle \theta^4 \rangle \approx \frac{8(3 - \gamma)}{3} \xi + \frac{4(\gamma^2 - 3)}{3} \xi^2 \pm \cdots , \tag{23}$$

to relate $\langle \theta^2 \rangle$ and $\langle \theta^4 \rangle$ to the quantities ξ and γ used in the present paper. Note that in the limit of infinitely high energies where $\gamma \to 3$, we have $\langle \theta^2 \rangle \approx 2\xi - \xi^2/3$ and $\langle \theta^4 \rangle \approx 8\xi^2$, i.e. our ξ corresponds to their X divided by two. We can therefore expand p_{corr} and p_{uncorr} in a power series of ξ, in analogy to their expansion in X:

$$p_{\text{corr}} = s(p_{0c} + p_{1c}\xi + p_{2c}\xi^2),$$
$$p_{\text{uncorr}} = s(p_{0u} + p_{1u}\xi + p_{2u}\xi^2). \tag{24}$$

With

$$\rho \approx \frac{1}{\sqrt{3}} + \rho_1 \xi \tag{25}$$

and the exact $\langle z \rangle$ and $\langle z^2 \rangle$ we obtain for the zeroth and first order coefficients

$$p_{0c} = \sqrt{3} - 1$$
$$p_{0u} = 2 - \sqrt{3}$$
$$p_{1u} = \frac{6 + 7\gamma}{27\sqrt{3}} - \frac{3 + 2\gamma}{18} - p_{1c}. \tag{26}$$

Note that these expressions differ significantly from the zeroth and first order coefficients found in Ref. [20]. We then have for the correlation moments

$$\langle z \cos \theta \rangle_{\text{FLUKA}} \approx s \left(1 - \frac{27 - 4\sqrt{3}(3 - \gamma)}{18} \xi \pm \cdots \right),$$
$$\langle x v_x + y v_y \rangle_{\text{FLUKA}} \approx s \left(\frac{30 - \gamma - 6\sqrt{3}(3 - \gamma)}{27} \xi \pm \cdots \right), \tag{27}$$

i.e. they agree with the exact ones only in the limit $\gamma \to 3$. If we consider this limit and go to $O(\xi^2)$, we obtain from $\langle z \rangle$

$$p_{2u} = \frac{18 - 17\sqrt{3}}{54} + \frac{p_{1c}}{3} - p_{2c} + 2\rho_1 \tag{28}$$

which leads to an over-estimated $\langle z^2 \rangle$:

$$\lim_{\gamma \to 3} \langle z^2 \rangle_{\text{FLUKA}} \approx s^2 \left(1 - \xi + \frac{11}{12} \xi^2 \pm \cdots \right) \tag{29}$$

independent of p_{1c}, p_{2c} and ρ_1. For $\gamma < 3$ it is possible to simultaneously describe $\langle z \rangle$ and $\langle z^2 \rangle$, however, the resulting expressions for p_{ic} and p_{iu} contain factors of the form $3 - \gamma$ in the denominator, i.e. they diverge at high energies.

It is possible to take another subset of moments to fix the parameters $p_{\text{corr}}, p_{\text{uncorr}}$ and ρ. If we use for instance the first order spatial moments and their correlations with the multiple scattering angle we get

$$\rho \approx \frac{1}{2}, \quad p_{0c} = 1, \quad p_{0u} = 0, \quad p_{1u} = -p_{1c} \tag{30}$$

resulting in

$$\langle z^2 \rangle_{\text{FLUKA}} \approx s^2 \left(1 - \frac{3+\gamma}{9} \xi \pm \cdots \right),$$
$$\langle x^2 + y^2 \rangle_{\text{FLUKA}} \approx s^2 \left(\frac{\gamma}{6} \xi \pm \cdots \right). \tag{31}$$

We see that the second order longitudinal moment agrees with the exact one in the limit $\gamma \to 3$. The second order transverse moment is under-estimated for every possible value of γ. By going to $O(\xi^2)$ we find again factors of the form $3 - \gamma$ in the denominators of the various expressions for p_{ic} and p_{iu}.

The above analysis suggests that it is not possible to describe simultaneously the first and second order spatial moments and their correlations with the multiple scattering angle using the approach proposed by Ferrari et al.

3.5. PENELOPE

Baro et al. [23] adopted a slightly modified version of the algorithm proposed by Berger in their electron transport Monte-Carlo code called PENELOPE [24]:

$$x = s\eta \, \sin \, \theta \, \cos \, \phi,$$
$$y = s\eta \, \sin \, \theta \, \sin \, \phi,$$
$$z = s(1 - \eta + \eta \, \cos \, \theta), \tag{32}$$

where η is a uniformly distributed random number between zero and unity. This modification leaves the first order moments unchanged but improves the second order moments:

$$\frac{\langle z^2 \rangle_{\text{PENELOPE}} - \langle z^2 \rangle}{\langle z^2 \rangle} = s^2 \frac{1 + \langle \cos \, \theta \rangle + \langle \cos^2 \theta \rangle}{3 \langle z^2 \rangle} - 1 \approx \frac{3 + 2\gamma(\gamma - 1)}{36} \xi^2 \pm \cdots \,,$$
$$\frac{\langle x^2 + y^2 \rangle_{\text{PENELOPE}} - \langle x^2 + y^2 \rangle}{\langle x^2 + y^2 \rangle} = \frac{s^2 \langle \sin^2 \theta \rangle}{3 \langle x^2 + y^2 \rangle} - 1 \approx -\frac{\gamma - 1}{4} \xi + \frac{3 - 12\gamma + 13\gamma^2}{240} \xi^2 \pm \cdots \tag{33}$$

Another advantage is that the final position of the particle is no longer bounded in the range $z > 0$ but can be anywhere in a sphere with a radius s. The overall accuracy of the algorithm is $O(\xi)$.

3.6. LLCA

Recently Kawrakow [25] developed an electron transport algorithm called LLCA (from **L**ongitudinal-and-**L**ateral-**C**orrelation-**A**lgorithm) which was shown to produce more step size stable results than

PRESTA. In this algorithm the final particle position is correlated to the scattering angle and calculated according to:

$$x = \bar{t} \sin \psi \cos (\phi + \tilde{\phi}),$$
$$y = \bar{t} \sin \psi \sin (\phi + \tilde{\phi}),$$
$$z = \bar{t} \cos \psi,$$
$$\cos \psi = 1 - \alpha(1 - \cos \theta). \tag{34}$$

Here, $\tilde{\phi}$ is the angle between the transverse components of the vectors of motion and position, respectively. This angle is sampled from a distribution pre-calculated by a single scattering Monte Carlo (SSMC). $\bar{t}$ is a short hand notation for $\sqrt{\langle x^2 + y^2 + z^2 \rangle}$ and α is taken such that $\langle z \rangle$ is described exactly, i.e.

$$\alpha = \frac{1 - \langle z \rangle / \bar{t}}{1 - \langle \cos \theta \rangle} \approx \frac{1}{3} \left(1 + \frac{\xi}{4} + \frac{\xi^2}{360} \pm \cdots \right). \tag{35}$$

It is clear that LLCA automatically describes $\langle z \rangle$ and the combined second order moment $\langle x^2 + y^2 + z^2 \rangle$. The correlation $\langle x v_x + y v_y \rangle$ cannot be calculated analytically because $\langle \cos \tilde{\phi} \rangle$ is known only numerically. For the longitudinal correlation function we get from Eq. (34)

$$\frac{\langle z v_z \rangle_{\text{LLCA}} - \langle z v_z \rangle}{\langle z v_z \rangle} = \frac{\bar{t}[(1 - \alpha)\langle \cos \theta \rangle + \alpha \langle \cos^2 \theta \rangle]}{\langle z v_z \rangle} - 1 \approx -\frac{3 - \gamma}{9} \xi + \frac{(\gamma - 3)(\gamma - 2)}{27} \xi^2 \pm \cdots, \tag{36}$$

that is, this function is over-estimated and correct only to $O(\xi)$. However, at high energies ($\gamma \to 3$), the longitudinal correlation function is correct up to $O(\xi^3)$.

For the second order moments we get

$$\frac{\langle z^2 \rangle_{\text{LLCA}} - \langle z^2 \rangle}{\langle z^2 \rangle} = \frac{\bar{t}^2 \left[(1 - \alpha)^2 + 2\alpha(1 - \alpha)\langle \cos \theta \rangle + \alpha^2 \langle \cos^2 \theta \rangle \right]}{\langle z^2 \rangle} - 1 \approx -4\frac{3 - \gamma}{27} \xi + \frac{81 - 57\gamma + 7\gamma^2}{486} \xi^2 \pm \cdots,$$
$$\frac{\langle x^2 + y^2 \rangle_{\text{LLCA}} - \langle x^2 + y^2 \rangle}{\langle x^2 + y^2 \rangle} = \frac{\bar{t}^2 \alpha [2 - \alpha - 2(1 - \alpha)\langle \cos \theta \rangle - \alpha \langle \cos^2 \theta \rangle]}{\langle x^2 + y^2 \rangle} - 1 \approx 2\frac{3 - \gamma}{3\gamma} - \frac{33 - 23\gamma + 3\gamma^2}{36\gamma} \xi^2 \pm \cdots, \tag{37}$$

i.e., $\langle z^2 \rangle$ is under-estimated and $\langle x^2 + y^2 \rangle$ is over-predicted. For $\gamma \to 3$ these moments are correct to $O(\xi^2)$.

3.7. Graphical representation

We conclude the analysis of presently available electron transport algorithms with a set of graphs depicting the moments analyzed in Sections 3.2–3.6. FLUKA's algorithm [20] is not included in the comparisons due to the fact that the various coefficients derived in this paper differ significantly from those derived in [20]. Results from the new algorithm presented in Section 4.4 are shown in order to demonstrate the strong improvement compared to the algorithms analyzed in Sections 3.2–3.6. In all cases the ratio of the moment resulting from the various algorithms to the exact moment, calculated from Eq. (2), is shown as a function of ξ. The maximum value of 0.5 for ξ chosen to plot the data roughly corresponds to an average multiple scattering angle of one radian and is considered to be the maximum value acceptable in a condensed history simulation of electron transport. Results for a simple condensed history algorithm (see Section 3.1) are not included in the figures in order to avoid a substantial expansion of the plot ranges which would make much more difficult or impossible to see the differences between the various algorithms.
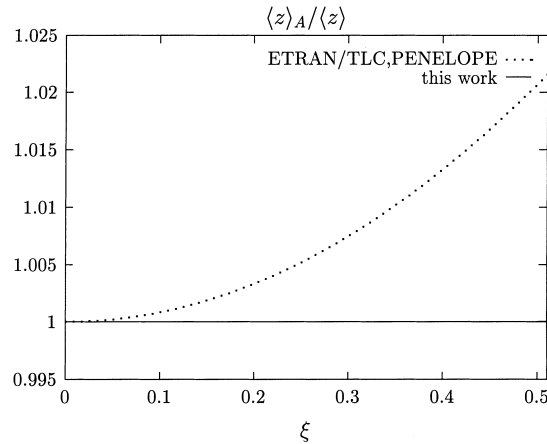
Fig. 2. The ratio of the average transport distance in the initial direction of motion $\langle z \rangle$ resulting from various algorithms to the exact expression given in Eq. (2). Both PRESTA and LLCA force this moment to be exact (see Sections 3.2 and 3.6) and are therefore not included in this figure.

In Fig. 2 the results for $\langle z \rangle$ are depicted. Because PRESTA and LLCA are constructed from the requirement that this moment is exactly reproduced they are not included in this figure. The algorithms of PENELOPE's and ETRAN/TLC produce identical results and over-estimate the average transport distance in the initial direction of motion by about 2% for $\xi = 0.5$. The maximum deviation from the exact answer for the new algorithm is 0.002%.

In Fig. 3 the results for $\langle zv_z \rangle$, the average correlation between the longitudinal component of the final direction of motion and the transport distance in the initial direction of motion, are shown for two different values of γ. The dependence of this and also all other moments on γ is rather weak and therefore it is sufficient to present results only for the two extreme situations: $\gamma \to 3$ (infinitely high energies) and $\gamma \to 1$ (very low energies). Due to the fact that in PRESTA the electrons are always transported by $\langle z \rangle$, independently of the sampled multiple scattering angle, this correlation function is under-estimated for all energies, the maximum deviation being 30% at $\xi = 0.5$ and $\gamma = 1$. ETRAN/TLC and PENELOPE produce again identical results $\langle zv_z \rangle$ being over-predicted at high energies and under-estimated at low energies. LLCA agrees with the exact answer within 0.1% at high energies but under-estimates the longitudinal correlation by 10% at $\xi = 0.5$ and $\gamma = 1$. The new algorithm reproduces the exact expression to better than 0.05% for all energies.

Results for the transverse correlation function $\langle xv_x + yv_y \rangle$ are shown in Fig. 4. LLCA is not included in this comparison for the reasons described in Section 3.6. PENELOPE and ETRAN/TLC are identical again. Note that PRESTA results will be lower than shown for $\xi \leqslant 0.295$ (see Section 3.2).

Results for the second longitudinal moment $\langle z^2 \rangle$ are represented in Fig. 5. PRESTA shows again the strongest variation with step size. From the moments studied, $\langle z^2 \rangle$ is the moment for which we observe the maximum deviation between the new algorithm described in Section 4.4 and the exact answer. This maximum deviation is achieved for $\xi = 0.5$ and $\gamma = 3$ and is 0.3%.

Finally we show in Fig. 6 the results for the average lateral transport $\langle x^2 + y^2 \rangle$. ETRAN/TLC is not included in the comparisons because it reproduces the correct answer, provided Eq. (21) is used to calculate the straggling functions δ_x and δ_y (see Section 3.3). Note also that PRESTA results will be lower than shown for $\xi \leqslant 0.295$ (see Section 3.2).
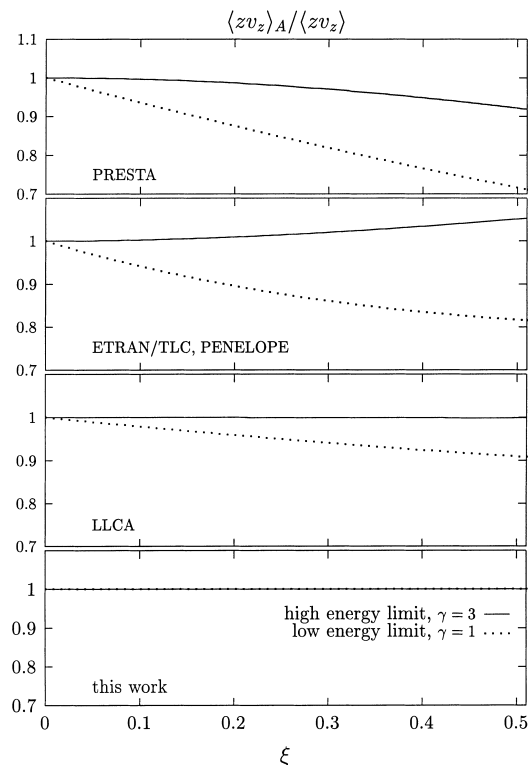
Fig. 3. The ratio, resulting from various algorithms to the exact expression given in Eq. (2), of the average correlation between the transport distance in the initial direction of motion and the longitudinal component of the final direction $\langle zv_z \rangle$.

4. New algorithms

In this section we will discuss ways of decreasing the order of the truncation error due to the use of the condensed history technique. We start with a general discussion in Section 4.1, analyze different ways of step subdivisions in Sections 4.2 and 4.3 and present the best solution we were able to find in Section 4.4.

4.1. General discussion

Larsen [2] studied the condensed history technique in an operator formalism and showed that this technique gets the correct answer in the limit of small step sizes providing that the exact theory is employed to describe multiple scattering. We will use Larsen's analysis to show that the sampling of at least two multiple scattering angles per electron step is required in order to improve the convergence of the condensed history technique to one additional order of the step length.

We can write Eq. (1) in the following form:

$$\frac{\partial}{\partial s} f(s; \vec{x}, \vec{v}) = -(A + B) f(s; \vec{x}, \vec{v}), \tag{38}$$

where A is the "streaming operator",

$$Af(s; \vec{x}, \vec{v}) = \vec{v} \vec{\nabla} f(s; \vec{x}, \vec{v}), \tag{39}$$

$$\langle xv_x + yv_y \rangle_A / \langle xv_x + yv_y \rangle$$
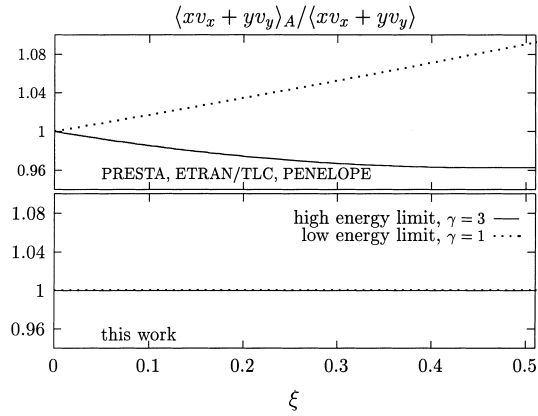
Fig. 4. The ratio, resulting from various algorithms to the exact expression given in Eq. (2), of the average correlation between lateral transport and the transverse component of the final direction, $\langle xv_x + yv_y \rangle$. Note that in reality PRESTA's results will be lower than shown for $\xi \leqslant 0.295$ (see Section 3.2).

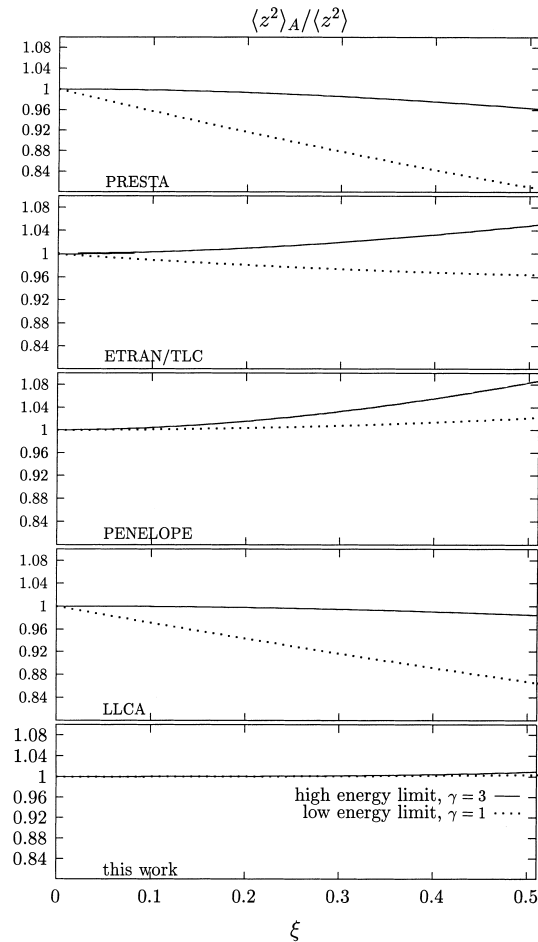$$\langle z^2 \rangle_A / \langle z^2 \rangle$$

Fig. 5. The ratio of the second longitudinal moment $\langle z^2 \rangle$ resulting from various algorithms to the exact expression given in Eq. (2).
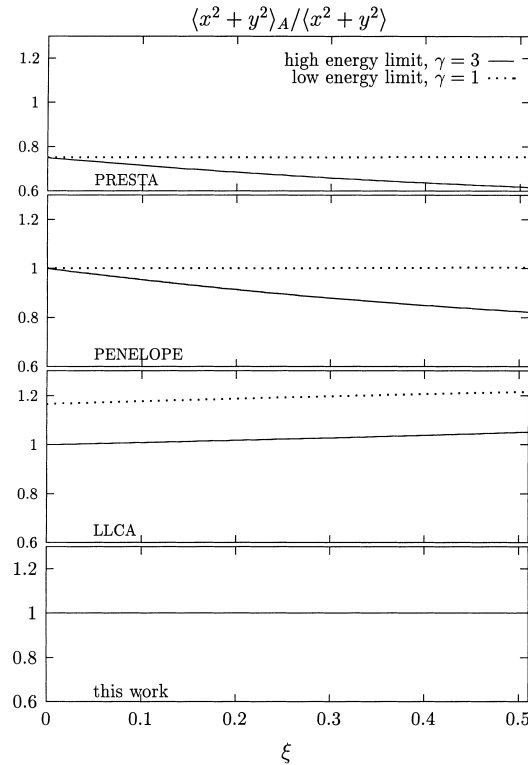
Fig. 6. The ratio of the second transverse moment $\langle x^2 + y^2 \rangle$ resulting from various algorithms to the exact expression given in Eq. (2). Note that in reality PRESTA's results will be lower than shown for $\xi \leqslant 0.295$ (see Section 3.2).

and B the "angular scattering" operator,

$$Bf(s;\vec{x},\vec{v}) = N \int d\vec{v} \left[f(\vec{x}, \vec{v'}, s) - f(\vec{x}, \vec{v}, s) \right] \sigma(\vec{v} \cdot \vec{v'}). \tag{40}$$

Eq. (38) has the formal solution

$$f(s;\vec{x},\vec{\Omega}) = \exp\left[-(A + B)s \right] f(0;\vec{x},\vec{\Omega}) \tag{41}$$

which, expanded in a power series of s, reads

$$f(s;\vec{x},\vec{v}) \approx \left(1 - (A+B)s + \frac{A^2 + AB + BA + B^2}{2} s^2 - \frac{A^3 + A^2 B + AB^2 + ABA + BAB + BA^2 + B^2 A + B^3}{6} s^3 \right.$$

$$\left. \pm \cdots \right) f(0;\vec{x},\vec{v}). \tag{42}$$

Berger's algorithm, for instance, corresponds to

$$f(s;\vec{x},\vec{v}) = \exp\left(-\frac{As}{2} \right) \exp(-Bs) \exp\left(-\frac{As}{2} \right) f(0;\vec{x},\vec{v}) \tag{43}$$

(i.e. transport the particle by $s/2$, sample a scattering angle from the distribution resulting from the whole step and rotate, and transport again by $s/2$). Expanded in a power series of s, the above equation gives

$$f(s;\vec{x},\vec{v}) \approx \left(1 - (A+B)s + \frac{A^2 + AB + BA + B^2}{2}s^2 - \left(\frac{A^3}{6} + \frac{A^2B}{8} + \frac{AB^2}{4} + \frac{ABA}{4} + \frac{B^2A}{4} + \frac{BA^2}{8} + \frac{B^3}{6}\right)s^3\right.$$

$$\left. \pm \cdots \right)f(0;\vec{x},\vec{v}). \tag{44}$$

In addition to the wrong coefficients for A^2B, AB^2, ABA and B^2A we are missing the term BAB. To get such a term, two or more factors of the form $\exp(\beta_iBs)$ are required. In other words, at least two multiple scattering angles per step have to be sampled in order to improve the convergence of the condensed history technique by one additional order of s.

Before we conclude this section it is interesting to note that the improvement achieved by the modification of Berger's algorithm used in PENELOPE can be observed also in Larsen's operator formalism. We have namely

$$\int_0^1 d\eta \, \exp(-\eta As) \, \exp(-Bs) \, \exp(-(1-\eta)As) \approx 1 - (A+B)s + \frac{A^2 + AB + BA + B^2}{2}s^2 - \left(\frac{A^3}{6} + \frac{A^2B}{6} + \frac{AB^2}{4}\right.$$

$$\left. + \frac{ABA}{6} + \frac{B^2A}{4} + \frac{BA^2}{6} + \frac{B^3}{6}\right)s^3 \pm \cdots, \tag{45}$$

i.e. now only the coefficients of AB^2 and B^2A are wrong.

4.2. Continuous integration

In the last section we have seen that at least two multiple scattering angles per step are required to obtain additional improvement of the condensed history technique. In general, there are two different ways to subdivide the step into two or more sub-steps: (i) use a fixed intermediate point and (ii) sample the intermediate point from a given distribution. In this subsection we will discuss the second possibility.

First of all, we note that we can rewrite Eq. (2) in the following manner:

$$\langle z \rangle = s \int_0^1 d\eta \langle \cos \theta(\eta s) \rangle$$

$$\langle z v_z \rangle = s \int_0^1 d\eta \langle \cos^2\theta(\eta s) \rangle \langle \cos \theta((1-\eta)s) \rangle$$

$$\langle x v_x + y v_y \rangle = s \int_0^1 d\eta \langle \sin^2\theta(\eta s) \rangle \langle \cos \theta((1-\eta)s) \rangle$$

$$\langle z^2 \rangle = s^2 \int_0^1 2\eta_1 \, d\eta_1 \int_0^1 d\eta_2 \langle \cos^2\theta(\eta_1\eta_2 s) \rangle k_1(\eta_1(1-\eta_2)s)$$

$$\langle x^2 + y^2 \rangle = s^2 \int_0^1 2\eta_1 d\eta_1 \int_0^1 d\eta_2 \langle \sin^2\theta(\eta_1\eta_2 s) \rangle k_1(\eta_1(1-\eta_2)s). \tag{46}$$

Here, $\langle \cos \theta(\eta s) \rangle$, for instance, means averaging the cosine of the scattering angle over the multiple scattering distribution evaluated for a step length of ηs. It is easy to construct a Monte Carlo algorithm that satisfies the first three equations:

A1 Sample a random number η uniformly distributed between zero and one.

A2 Sample θ_1 from the multiple scattering distribution $f(\eta s; \cos \theta)$ and ϕ_1 uniformly distributed between zero and 2π.

A3 Sample θ_2 from the multiple scattering distribution $f((1-\eta)s; \cos \theta)$ and ϕ_2 uniformly distributed between zero and 2π.

A4 Take the final scattering angle and co-ordinates to be:

$$
\begin{aligned}
v_z &= \cos \theta = \cos \theta_1 \cos \theta_2 - \sin \theta_1 \sin \theta_2 \cos \phi_2, \\
v_x &= \sin \theta \cos \phi = \sin \theta_2(\cos \theta_1 \cos \phi_1 \cos \phi_2 - \sin \phi_1 \sin \phi_2) + \cos \theta_2 \sin \theta_1 \cos \phi_1, \\
v_y &= \sin \theta \sin \phi = \sin \theta_2(\cos \theta_1 \sin \phi_1 \cos \phi_2 + \cos \phi_1 \sin \phi_2) + \cos \theta_2 \sin \theta_1 \sin \phi_1, \\
z &= s \cos \theta_1, \\
x &= s \sin \theta_1 \cos \phi_1, \\
y &= s \sin \theta_1 \sin \phi_1.
\end{aligned}
\tag{47}
$$

It can be shown that this procedure satisfies also higher order correlation functions $\langle zv_z^n \rangle$ and $\langle xv_x^n \rangle$. Unfortunately, the second order spatial moments $\langle z^2 \rangle$ and $\langle x^2 + y^2 \rangle$ are over-estimated. We have $x^2 + y^2 + z^2 = s^2$ (i.e. the particle is always on a sphere with the radius s, whereas in reality the particle can be somewhere within this sphere) and also:

$$
\langle z^2 \rangle = s^2 \int_0^1 d\eta \langle \cos^2\theta(\eta s) \rangle \approx s^2 \left(1 - \frac{\gamma}{3}\xi + \frac{\gamma^2}{9}\xi^2 \pm \cdots \right),
$$

$$
\langle x^2 + y^2 \rangle = s^2 \int_0^1 d\eta \langle \sin^2\theta(\eta s) \rangle \approx s^2 \left(\frac{\gamma}{3}\xi - \frac{\gamma^2}{9}\xi^2 \pm \cdots \right).
\tag{48}
$$

We can try to improve the situation by undertaking one additional subdivision. Then three scattering angles have to be sampled from $f(\eta_1\eta_2 s; \cos \theta)$, $f(\eta_1(1-\eta_2)s; \cos \theta)$ and $f((1-\eta_1)s; \cos \theta)$, respectively. Here, η_1 is chosen from $2\eta_1 d\eta_1$ and η_2 from $d\eta_2$. In order to satisfy the first three equations of (46) the co-ordinates have to be calculated according to

$$
\begin{aligned}
z &= \frac{s}{2}(\cos \theta_1 + \cos \theta_1 \cos \theta_2 - \sin \theta_1 \sin \theta_2 \cos \phi_2), \\
x &= \frac{s}{2}(\sin \theta_1 \cos \phi_1 + \sin \theta_2(\cos \theta_1 \sin \phi_1 \cos \phi_2 - \cos \phi_1 \sin \phi_2) + \cos \theta_2 \sin \theta_1 \cos \phi_1), \\
y &= \frac{s}{2}(\sin \theta_1 \sin \phi_1 + \sin \theta_2(\cos \theta_1 \sin \phi_1 \cos \phi_2 + \cos \phi_1 \sin \phi_2) + \cos \theta_2 \sin \theta_1 \sin \phi_1).
\end{aligned}
\tag{49}
$$

With this we have for the second order moments

$$
\langle z^2 \rangle = \frac{s^2}{4} \int_0^1 2\eta_1 \, d\eta_1 \int_0^1 d\eta_2 \left[\langle \cos^2\theta(\eta_1\eta_2 s) \rangle + \langle \cos^2\theta(\eta_1 s) \rangle + 2\langle \cos^2\theta(\eta_1\eta_2 s) \rangle \langle \cos \theta(\eta_1(1-\eta_2)s) \rangle \right]
$$

$$
\approx s^2 \left(1 - \frac{3+5\gamma}{9}\xi + \frac{3+2\gamma+6\gamma^2}{72}\xi^2 \pm \cdots \right),
$$

$$\langle x^2 + y^2 \rangle = \frac{s^2}{4} \int_0^1 2\eta_1 \, d\eta_1 \int_0^1 d\eta_2 \left[\langle \sin^2\theta(\eta_1\eta_2 s) \rangle + \langle \sin^2\theta(\eta_1 s) \rangle + 2\langle \sin^2\theta(\eta_1\eta_2 s) \rangle \langle \cos \theta(\eta_1(1-\eta_2)s) \rangle \right]$$

$$\tag{50}$$

$$\approx s^2 \left(\frac{5\gamma}{18}\xi - \frac{\gamma(1+3\gamma)}{36}\xi^2 \pm \cdots \right),$$

i.e. they are again over-estimated. If we calculate the difference between the exact Lewis' moments and the moments resulting from one or two subdivisions, $\langle z^2, x^2 + y^2 \rangle_1$ or $\langle z^2, x^2 + y^2 \rangle_2$, we obtain

$$\langle z^2 \rangle_1 - \langle z^2 \rangle = \frac{3-\gamma}{9}\xi \pm \cdots, \qquad \langle x^2 + y^2 \rangle_1 - \langle x^2 + y^2 \rangle = \frac{\gamma}{9}\xi \pm \cdots ,$$

$$\langle z^2 \rangle_2 - \langle z^2 \rangle = \frac{3-\gamma}{18}\xi \pm \cdots, \qquad \langle x^2 + y^2 \rangle_2 - \langle x^2 + y^2 \rangle = \frac{\gamma}{18}\xi \pm \cdots .$$

$$\tag{51}$$

The above procedure can be generalized to N subdivisions of the electron step. To satisfy the first order spatial moments and their correlations with the final direction of motion we have to calculate the final co-ordinates according to

$$\vec{x} = \frac{s}{N} \sum_{i=1}^{N} \vec{\Omega}_i \tag{52}$$

where $\vec{\Omega}_i$ is the direction of motion after i subsequent scattering with the scattering angles $\theta_1, \ldots, \theta_i$ sampled from the multiple scattering distributions $f(\eta_1\eta_2 \ldots \eta_N s; \cos \theta), f(\eta_2 \ldots \eta_N s; \cos \theta), \ldots, f(\eta_i \ldots \eta_N s; \cos \theta)$. Here, $\eta_1, \eta_2, \ldots, \eta_N$ are random numbers distributed according to $N\eta_1^{(N-1)}d\eta_1, (N-1)\eta_2^{(N-2)}d\eta_2, \ldots, d\eta_N$. The difference between the second order moments resulting from N subdivisions and the exact ones turns out to be

$$\langle z^2 \rangle_N - \langle z^2 \rangle = \frac{3-\gamma}{9N}\xi \pm \cdots, \qquad \langle x^2 + y^2 \rangle_N - \langle x^2 + y^2 \rangle = \frac{\gamma}{9N}\xi \pm \cdots \tag{53}$$

Indeed, by going to very big N's the difference goes to zero as $1/N$ (this is true also for higher order terms in ξ). However, this is equivalent to a SSMC, i.e. there is no gain of CPU time.

We tried to construct a Monte Carlo algorithm starting from the second order moments. Looking at the last two equations of Eq. (46) we see that the following procedure will give an exact description of $\langle z^2 \rangle$ and $\langle x^2 + y^2 \rangle$:

  B1 Sample a random number η_1 from $2\eta_1 d\eta_1$ and a random number η_2 from $d\eta_2$, both between zero and unity.

  B2 Sample θ_1 from $f(\eta_1\eta_2 s; \cos \theta)$ and θ_2 from $f((1-\eta_1\eta_2)s; \cos \theta)$.

  B3 Calculate the final direction of motion from θ_1, ϕ_1 and θ_2, ϕ_2 (see Eq. (47)), and the final co-ordinates according to:

$$z = s\sqrt{k_1(\eta_1(1-\eta_2)s)} \cos \theta_1,$$

$$x = s\sqrt{k_1(\eta_1(1-\eta_2)s)} \sin \theta_1 \cos \phi_1, \tag{54}$$

$$y = s\sqrt{k_1(\eta_1(1-\eta_2)s)} \sin \theta_1 \sin \phi_1.$$

This algorithm will give for the first order moments and their correlations to the final scattering angle

$$\langle z \rangle = s \int_0^1 2\eta_1 \, \mathrm{d}\eta_1 \int_0^1 \mathrm{d}\eta_2 \sqrt{k_1(\eta_1(1-\eta_2)s)} \langle \cos \theta(\eta_1 \eta_2 s) \rangle \approx s \left(1 - \frac{\xi}{2} + \frac{7\xi^2}{48} \pm \cdots \right),$$

$$\langle z \cos \theta \rangle = s \int_0^1 2\eta_1 \, \mathrm{d}\eta_1 \int_0^1 \mathrm{d}\eta_2 \sqrt{k_1(\eta_1(1-\eta_2)s)} \langle \cos^2\theta(\eta_1 \eta_2 s) \rangle \langle \cos \theta((1-\eta_1\eta_2)s) \rangle$$

$$\approx s \left(1 - \frac{15 + 4\gamma}{18} \xi + \frac{57 + 20\gamma + 8\gamma^2}{144} \xi^2 \pm \cdots \right), \qquad (55)$$

$$\langle x \sin \theta \cos \phi \rangle = \frac{s}{2} \int_0^1 2\eta_1 \, \mathrm{d}\eta_1 \int_0^1 \mathrm{d}\eta_2 \sqrt{k_1(\eta_1(1-\eta_2)s)} \langle \sin^2\theta(\eta_1\eta_2 s) \rangle \langle \cos \theta((1-\eta_1\eta_2)s) \rangle$$

$$\approx s \left(\frac{\gamma}{9} \xi - \frac{\gamma(5 + 2\gamma)}{72} \xi^2 \pm \cdots \right),$$

i.e. they are all under-estimated. One could think of replacing $\sqrt{k_1(\eta_1(1-\eta_2)s)}$ in Eq. (54) by a distributed quantity $\bar{t}$ with $\langle \bar{t}^2 \rangle = k_1(\eta_1(1-\eta_2)s)$. However, in this case $\langle \bar{t} \rangle < \sqrt{k_1(\eta_1(1-\eta_2)s)}$ and the under-prediction of the first order moments will be even stronger.

4.3. N-point integration

To perform the integration in the first Eq. of (46), for instance, one also could use N-point numerical integration. As an example, Cotes formula,

$$\langle z \rangle = s \left(\frac{1}{6} + \frac{2}{3} \langle \cos \theta(s/2) \rangle + \frac{1}{6} \langle \cos \theta(s) \rangle \right), \qquad (56)$$

suggests the following relation between scattering angles and final co-ordinates:

$$z = \frac{s}{6}[1 + 4 \cos \theta_1 + \cos \theta],$$

$$x = \frac{s}{6}[4 \sin \theta_1 \cos \phi_1 + \sin \theta \cos \phi], \qquad (57)$$

$$y = \frac{s}{6}[4 \sin \theta_1 \sin \phi_1 + \sin \theta \cos \phi],$$

where θ_1 is the angle sampled from $f(s/2; \cos \theta)$ and θ the final scattering angle resulting from θ_1, ϕ_1 and θ_2, ϕ_2 (θ_2 is the multiple scattering angle for the substep $s/2 \ldots s$). This procedure describes $\langle z \rangle$, $\langle z v_z^n \rangle$ and $\langle x v_x^n \rangle$ up to $O(\xi^4)$. Looking again at the second order moments, we get:

$$\langle z^2 \rangle = \frac{s^2}{36} \left[1 + 16\langle \cos^2\theta(s/2) \rangle + \langle \cos^2\theta(s) \rangle + 8\langle \cos \theta(s/2) \rangle + 2\langle \cos \theta(s) \rangle + 8\langle \cos^2\theta(s/2) \rangle \langle \cos \theta(s/2) \rangle \right]$$

$$\approx s^2 \left(1 - \frac{15 + 13\gamma}{54} \xi + \frac{9 + 4\gamma + 7\gamma^2}{108} \xi^2 \pm \cdots \right),$$

$$\langle x^2 + y^2 \rangle = \frac{s^2}{36} \left[16\langle \sin^2\theta(s/2) \rangle + \langle \sin^2\theta(s) \rangle + 8\langle \sin^2\theta(s/2) \rangle \langle \cos \theta(s/2) \rangle \right] \approx s^2 \left(\frac{13\gamma}{54} \xi - \frac{\gamma(4 + 7\gamma)}{108} \xi^2 \pm \cdots \right)$$

$$(58)$$

they are over-estimated again. One could think that using a generalized formula,

$$\vec{x} = s\sum_{i=0}^{N}\alpha_i\vec{\Omega}(\beta_i s), \qquad N \geqslant 2, \tag{59}$$

there will be enough freedom to choose the coefficients α_i and the intermediate points $\beta_i s$ such that all first and second order moments are reproduced. However, it turns out that after using the first three equations of Eq. (46) to fix three of the free parameters, there is no real solution of the equation

$$\left(\sum_{i=0}^{N}\alpha_i\vec{\Omega}(\beta_i s)\right)_z^2 = \langle z^2\rangle! \tag{60}$$

The best we can do is to minimize the difference between the resulting second order moments and the exact ones. The minimization has a unique solution

$$\beta_i = \frac{i}{N}, \quad \alpha_0 = \alpha_N = \frac{1}{2(N+1)}, \quad \alpha_1 = \alpha_2 = \ldots = \alpha_{N-1} = \frac{N}{N^2-1}. \tag{61}$$

Using these values for the intermediate points and the coefficients, we get for the difference between the second order spatial moments resulting from Eq. (59) and the exact second order moments:

$$\langle z^2\rangle_N - \langle z^2\rangle \approx s^2\frac{3-\gamma}{18(N^2-1)}\xi \pm \cdots,$$

$$\langle x^2 + y^2\rangle_N - \langle x^2 + y^2\rangle \approx s^2\frac{\gamma}{18(N^2-1)}\xi \pm \cdots \tag{62}$$

It is remarkable to observe that the N-point integration procedure shows a faster convergence then the continuous integration discussed in the last subsection!

Larsen [2] stated that the process of "mixing" the order of the streaming and scattering processes over several steps can clearly be generalized to yield higher order truncation error of the condensed history technique. We did not find a general proof for or against this statement, however, the discussion of the last two subsections seems to indicate that there is no possible representation of the operator $\exp(-(A+B)s)$ of the form $\prod \exp(-\alpha_i P_s s)$, where P_i is either A or B and the alpha's are numbers with $\sum \alpha_i = 1$, which gives an $O(s^4)$ error. Thus, some more elaborate methods are required to improve the convergence of the condensed history technique.

4.4. The best solution found

Let us consider a step subdivision with one intermediate point at $s/2$ and scattering angles θ_1, ϕ_1 and θ_2, ϕ_2. If we relate the final co-ordinates to these scattering angles according to:

$$z = s\left[\frac{1}{6} + \left(\frac{1}{3}+\delta\right)\cos\theta_1 + \left(\frac{1}{3}-\delta\right)\cos\theta_2 + \frac{1}{6}\cos\theta\right),$$

$$x = s\left[\left(\frac{1}{3}+\delta\right)\sin\theta_1\cos\phi_1 + \left(\frac{1}{3}-\delta\right)\sin\theta_2(\cos\phi_1\cos\phi_2 - \cos\theta_1\sin\phi_1\sin\phi_2) + \frac{1}{6}\sin\theta\cos\phi\right],$$

$$y = s\left[\left(\frac{1}{3}+\delta\right)\sin\theta_1\sin\phi_1 + \left(\frac{1}{3}-\delta\right)\sin\theta_2(\sin\phi_1\cos\phi_2 + \cos\theta_1\cos\phi_1\sin\phi_2) + \frac{1}{6}\sin\theta\sin\phi\right], \tag{63}$$

the first order moments and their correlations with the final scattering angle θ, ϕ will be correct up to $O(\xi^4)$. The remaining free parameter δ can be fixed from one of the second order moments. If we use for instance $\langle x^2 + y^2\rangle$ we obtain for δ

$$\delta = \frac{1}{2\sqrt{3}}\left(1 - \frac{6 - (5 - 2\sqrt{3})\gamma}{36}\xi \pm \cdots\right) \tag{64}$$

reproducing in this way $\langle x^2 + y^2\rangle$ with an $O(\xi^3)$ error. With this δ we get for the second order longitudinal moment

$$\langle z^2\rangle_A \approx s^2\left(1 - \frac{3 + 2\gamma}{9}\xi + \frac{36 + (66 - 12\sqrt{3})\gamma + (29 + 4\sqrt{3})\gamma^2}{648}\xi^2 \pm \cdots\right) \tag{65}$$

i.e., $\langle z^2\rangle$ is automatically correct to $O(\xi)$. The subscript A indicates moments resulting from the proposed algorithm. It is worth noticing that for $\xi \leqslant 1/2$ (this is the maximum step length considered acceptable in a condensed history simulation of electron transport and also the maximum step size for which a recently developed exact multiple scattering theory has been implemented [26]) the maximum difference between $\langle z^2\rangle$ resulting from the proposed algorithm and the exact one is below 0.3%, i.e. of the same order as numerical uncertainties due to interpolations during the sampling of the multiple scattering angles. To see this, let us consider two extreme situations: (i) transport at very low energies where $\gamma \to 1$ and (ii) transport at very high energies where

$$\gamma \approx 3 - \zeta, \qquad \zeta = \frac{3\langle\theta^4\rangle}{4\langle\theta^2\rangle} \ll 1. \tag{66}$$

We have then:

case (i): $\dfrac{\langle z^2\rangle_A - \langle z^2\rangle}{\langle z^2\rangle} \approx -0.0136\xi^2 \pm \cdots$,

case (ii): $\dfrac{\langle z^2\rangle_A - \langle z^2\rangle}{\langle z^2\rangle} \approx (0.0189 - 0.0135\zeta)\xi^2 \pm \cdots$ \hfill (67)

There is no way of representing Eq. (63) as a series of subsequent particle transport and scattering processes. Therefore, we cannot use Larsen's operator formalism to study the truncation error of this algorithm. From the moments studied above we can conclude that the truncation error is $O(s^4)$. [3] In principle it is possible to study arbitrary high order moments using Lewis' method. However, the resulting expressions become more and more complicated with increasing order of the moments. So, we could not find a general proof that the truncation error of the algorithm presented above is $O(s^4)$. It is worth giving the next few higher order moments. We have

$$\langle z^2 v_z\rangle = \frac{2}{3}\int_0^s \mathrm{d}s' k_1(s - s')\int_0^{s'} \mathrm{d}s''\left[k_1(s'') + \frac{2}{5}k_2(s' - s'')(2k_1(s'') + 3k_3(s''))\right]$$

$$\approx s^2\left(1 - \frac{2(12 + 5\gamma + 3\gamma_3)}{45}\xi + \frac{33 + 14\gamma + 10\gamma^2 + 6\gamma_3(1 + \gamma + \gamma_3)}{180}\xi^2 \pm \cdots\right), \tag{68}$$

where we have defined $\gamma_3 = \kappa_3/\kappa_1$. The proposed algorithm yields

---

[3] To be consistent with Larsen's definition of truncation error [2] we have to consider absolute instead of relative errors. First order moments have therefore a truncation error proportional to $s\xi^4$ and if we remember that $\xi \propto s$, it is clear that the truncation error is $O(s^5)$. The truncation error of second order moments is proportional to $s^2\xi^2$ (longitudinal) or $s^2\xi^3$ (transversal) and thus $O(s^4)$. The truncation error of fourth or higher order moments is automatically $O(s^4)$ or higher as such moments are proportional to at least s^4.

$$\langle z^2 v_z \rangle_A \approx s^2 \left(1 - \frac{2(12 + 5\gamma + 3\gamma_3)}{45} \xi \right.$$
$$\left. + \frac{801 + \gamma(48\sqrt{3} - 72) + \gamma^2(150 - 40\sqrt{3}) + \gamma_3(54 + \gamma(66 + 12\sqrt{3}) + 9\gamma_3)}{3240} \xi^2 \pm \cdots \right). \tag{69}$$

We observe again an $O(\xi)$ agreement between both expressions. Although the second order terms look completely different, they have almost the same value. The maximum deviation between both is well below 1% for $\xi \leqslant 1/2$. To show this, we consider again the two extreme situations discussed above and obtain:

case (i): $\quad \dfrac{\langle z^2 v_z \rangle_A - \langle z^2 v_z \rangle}{\langle z^2 v_z \rangle} \approx 0.02 \xi^2 \pm \cdots \;,$

case (ii): $\quad \dfrac{\langle z^2 v_z \rangle_A - \langle z^2 v_z \rangle}{\langle z^2 v_z \rangle} \approx (0.0139 - 0.0321\zeta)\xi^2 \pm \cdots \tag{70}$

In case (ii) we have made use of $\gamma_3 = 6 - 5\zeta$. Further we have

$$\langle z^2 v_z^2 \rangle = \frac{2}{9} \int_0^s ds' \left[1 + \frac{4}{5} k_2(s - s') \right] \int_0^{s'} ds'' k_1(s' - s'') \left[1 + 2k_2(s'') \right]$$
$$+ \frac{12}{105} \int_0^s ds' k_2(s - s') \int_0^{s'} ds'' k_3(s' - s'') \left[3k_2(s'') + 4k_4(s'') \right] \approx s^2 \left(1 - \frac{63 + 130\gamma + 42\gamma_3 + 24\gamma_4}{315} \xi \right. \tag{71}$$
$$\left. + \frac{189 + 210\gamma + 500\gamma^2 + 180\gamma\gamma_3 + 126\gamma_3^2 + 72\gamma_4(\gamma + \gamma_3 + \gamma_4)}{3780} \xi^2 \pm \cdots \right)$$

with $\gamma_4 = \kappa_4/\kappa_1$. From Eq. (63) we get

$$\langle z^2 v_z^2 \rangle_A \approx s^2 \left(1 - \frac{63 + 130\gamma + 42\gamma_3 + 24\gamma_4}{315} \xi \pm \cdots \right) \tag{72}$$

(we don't show here the second order term because of its length). Comparing again for case (i) and (ii) we have:

case (i): $\quad \dfrac{\langle z^2 v_z^2 \rangle_A - \langle z^2 v_z^2 \rangle}{\langle z^2 v_z^2 \rangle} \approx -0.0057 \xi^2 \pm \cdots \;,$

case (ii): $\quad \dfrac{\langle z^2 v_z^2 \rangle_A - \langle z^2 v_z^2 \rangle}{\langle z^2 v_z^2 \rangle} \approx (0.0139 - 0.0506\zeta)\xi^2 \pm \cdots \tag{73}$

We conclude the comparison of moments with the expressions for the third order longitudinal moment:

$$\langle z^3 \rangle = 2 \int_0^s ds' \int_0^{s'} ds'' k_1(s' - s'') \int_0^{s''} ds''' \left[k_1(s''') + \frac{2}{5} k_2(s'' - s''')(2k_1(s''') + 3k_3(s''')) \right]$$
$$\approx s^2 \left(1 - \frac{12 + 5\gamma + 3\gamma_3}{30} \xi + \frac{33 + 14\gamma + 10\gamma^2 + 6\gamma_3(1 + \gamma + \gamma_3)}{300} \xi^2 \pm \cdots \right). \tag{74}$$

The proposed algorithm again yield the exact moment to $O(\xi)$. Using the two extreme cases to compare the second order terms we have:

case (i): $\dfrac{\langle z^3 \rangle_A - \langle z^3 \rangle}{\langle z^3 \rangle} \approx 0.02\xi^2 \pm \cdots$,

case (ii): $\dfrac{\langle z^3 \rangle_A - \langle z^3 \rangle}{\langle z^3 \rangle} \approx 0.0194\zeta\xi^2 \pm \cdots$ (75)

Eq. (63) has one obvious disadvantage: the final longitudinal position z is bounded to the interval $-5/6s \leqslant z \leqslant s$ whereas in reality z can take values between $-s$ and s. To avoid this problem, the fixed coefficients in Eq. (63) can be replaced by distributed quantities:

$$z = s[\eta_0 + \eta_1 \, \cos \, \theta_1 + \eta_2 \, \cos \, \theta_2 + (1 - \eta_0 - \eta_1 - \eta_2) \, \cos \, \theta],$$
$$x = s[\eta_1 \, \sin \, \theta_1 \, \cos \, \phi_1 + \eta_2 \, \sin \, \theta_2(\cos \, \phi_1 \, \cos \, \phi_2 - \cos \, \theta_1 \, \sin \, \phi_1 \, \sin \, \phi_2) + (1 - \eta_0 - \eta_1 - \eta_2) \, \sin \, \theta \, \cos \, \phi],$$
$$y = s[\eta_1 \, \sin \, \theta_1 \, \sin \, \phi_1 + \eta_2 \, \sin \, \theta_2(\sin \, \phi_1 \, \cos \, \phi_2 + \cos \, \theta_1 \, \cos \, \phi_1 \, \sin \, \phi_2) + (1 - \eta_0 - \eta_1 - \eta_2) \, \sin \, \theta \, \sin \, \phi].$$
                                                                                                                                                         (76)

The coefficients η_i must then satisfy

$$\langle \eta_0 \rangle = \frac{1}{6}, \qquad \langle \eta_1 + \eta_2 \rangle = \frac{2}{3},$$ (77)

in order to reproduce the first order spatial moments to $O(\xi^4)$. From the $O(\xi)$ term of the second order moments we derive the following condition

$$\langle (\eta_0 + \eta_1)^2 \rangle + \langle (\eta_0 + \eta_2)^2 \rangle = \frac{2}{3} + O(\xi).$$ (78)

This procedure can be continued to higher order terms in ξ, however, the expressions become more and more complicated and will not be given here for the sake of brevity.

There are many different distributions in the variables η_i which simultaneously satisfy Eqs. (77) and (78). This gives us one additional degree of freedom to optimize not only the description of the spatial moments but also the resulting spatial distribution. Several distributions have been investigated until we decided to use the following form of the coefficients:

$$\eta_0 = (1 - \eta)/2,$$
$$\eta_1 = \eta\delta,$$
$$\eta_2 = \eta(1 - \delta),$$ (79)

where η is sampled from $2\eta \, \mathrm{d}\eta$ in the interval $0 \leqslant \eta \leqslant 1$. The parameter δ is given now by

$$\delta = \frac{1}{2} + \frac{\sqrt{6}}{6} - \left(\frac{1}{4\sqrt{6}} - \gamma \frac{4 - \sqrt{6}}{24\sqrt{6}} \right) \xi \pm \, .$$ (80)

5. An example

In this section we will present a simple example which demonstrates that the proposed lateral correlation algorithm approximates very closely the exact solution. A more detailed study of step size stability of the new algorithm will be presented elsewhere.

We consider electrons in an infinite homogeneous phantom starting at the origin and moving initially in z-direction. Not to obscure the results, all physical processes except elastic scattering are "turned off". Single elastic scattering is described for simplicity by the screened Rutherford cross section with a screening parameter χ_a. For this single scattering cross section an exact multiple scattering theory (without a small

angle approximation) applicable for all step sizes has been recently found [26]. We will be interested in the probability distributions $F_z(t;z)$ to find the electron at longitudinal position z after traveling a curved path length of t and $F_r(t;r)$ to find the electron at lateral displacement r. To characterize the correlation between final position and final direction of motion, we define the variable y,

$$y = \sqrt{\frac{1}{2\lambda\chi_a^2}}\left(\sqrt{1 - \cos\theta} - \sqrt{1 - \frac{z}{t}}\right),$$ (81)

λ being the number of mean free paths corresponding to path length t, and calculate the probability distribution $F_y(t;y)$ to find the electron having a correlation y. [4] The above distributions are calculated by sampling the final co-ordinates according to the algorithm presented in the last section and compared to a SSMC. To demonstrate the improvement compared to previously proposed algorithms, distributions resulting from them are also included. The new multiple scattering theory described in [26] has been used in all condensed history calculations to isolate the differences to geometrical transport methods only. Also, to make the comparison "fair", the other algorithms are allowed to take the transport distance in two steps. (since the new algorithm samples two multiple scattering angles per step and this is the most computationally intensive part of an electron transport algorithm, approximately the same CPU time is required for all condensed history calculations). LLCA results are not included in the comparisons as they have been discussed in Ref. [25] and also because the LLCA algorithm has not been implemented in a general purpose Monte Carlo code. FLUKA's algorithm [20] is not included as well due to the fact that the various coefficients derived in this paper differ significantly from those derived in [20].

In Fig. 7 we show the longitudinal distribution $F_z(z,t)$ for 128 keV electrons in gold and a path-length t corresponding to approximately 10 mean free paths and $\xi \approx 0.5$. Circles with error bars represent the single scattering result, line with dots corresponds to PRESTA, dashed line with circles to ITS/MCNP, long dashed line to the algorithm proposed by Berger and implemented by Seltzer as TLC, dashed line to PENELOPE and the full line to the algorithm proposed in this paper. Only our algorithm and PENELOPE "fill-in" the backscatter part of the distribution, PENELOPE's algorithm approaching even better the single scattering result in the extreme backward direction. However, in the more probable forward part of the distribution, our algorithm reproduces almost perfectly the result of the analog simulation. This is demonstrated in Fig. 8 where the same distribution as in Fig. 7 is shown but on a linear scale and only in the range $z/t > 0.6$ to allow for a better resolution of the various distributions.

In Fig. 9 the radial distribution for the same situation and with the same symbols as in the previous figure is depicted. The singularity in the PRESTA result was reported in Ref. [25]. Berger's algorithm has a similar singular behavior after 1 sub-step, however, due to longitudinal straggling the singularity is not so pronounced after two sub-steps. The distribution resulting from ITS/MCNP's algorithm is not shown because it does not fit in the plot scale chosen. Again, PENELOPE and the new algorithm are very close to the analog simulation, the new algorithm slightly outperforming PENELOPE in the region $r/t \to 1$.

The distribution in the position-direction correlation variable y is shown in Fig. 10. Here, the agreement between the analog simulation and the new algorithm is excellent. PRESTA and ITS/MCNP are again very far from the correct answer. PENELOPE and TLC show almost identical behavior being not too far from the single scattering result.

---

[4] It has been found empirically that $F_y(t;y)$ is nearly independent on the path-length t and screening parameter χ_a.
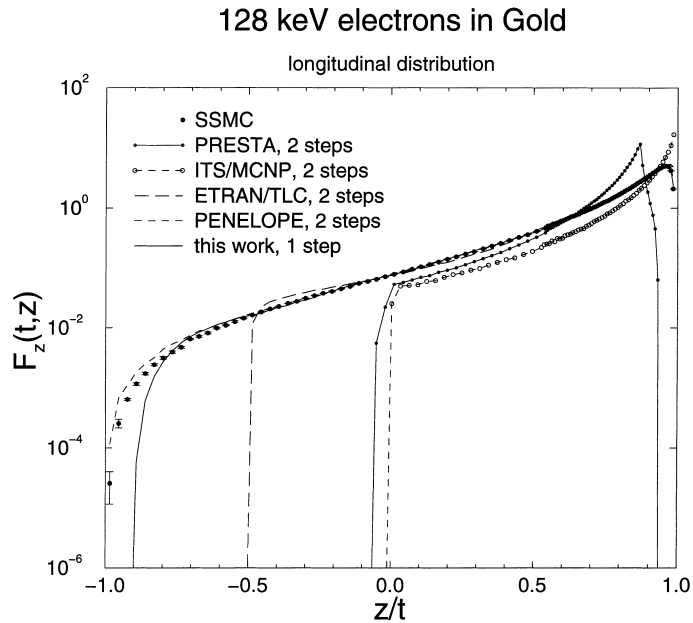
128 keV electrons in Gold

Fig. 7. The longitudinal distribution $F_z(t,z)$ of 128 keV electrons in gold starting at the origin and moving initially in the positive z direction after a path-length t corresponding to 10 elastic collisions ($\xi = 0.5$). Points with error bars correspond to the single scattering calculation, line with dots to PRESTA, dashed line with circles to ITS/MCNP, long dashed line to ETRAN/TLC, short dashed line to PENELOPE and the full line to the algorithm proposed in Section 4.4.

128 keV electrons in Gold
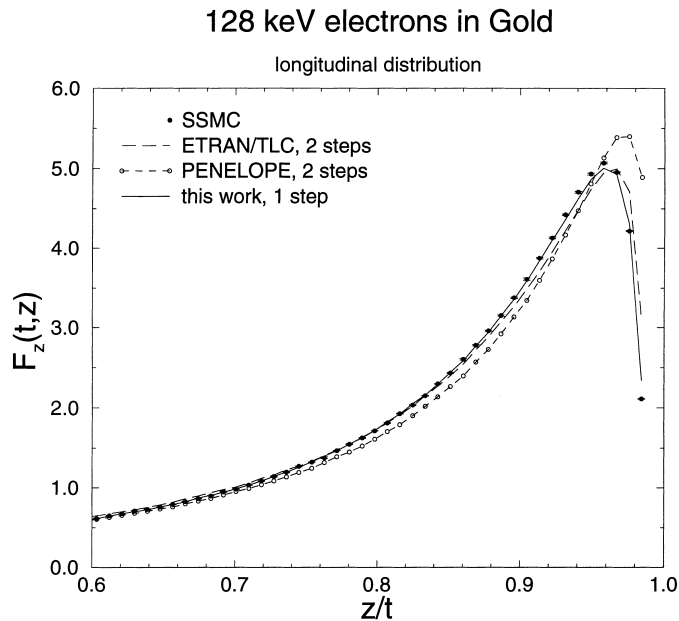
Fig. 8. The same as in Fig. 7 but plotted on a linear scale in the range $z/t > 0.6$ only to better visualize the various distributions in the forward region.
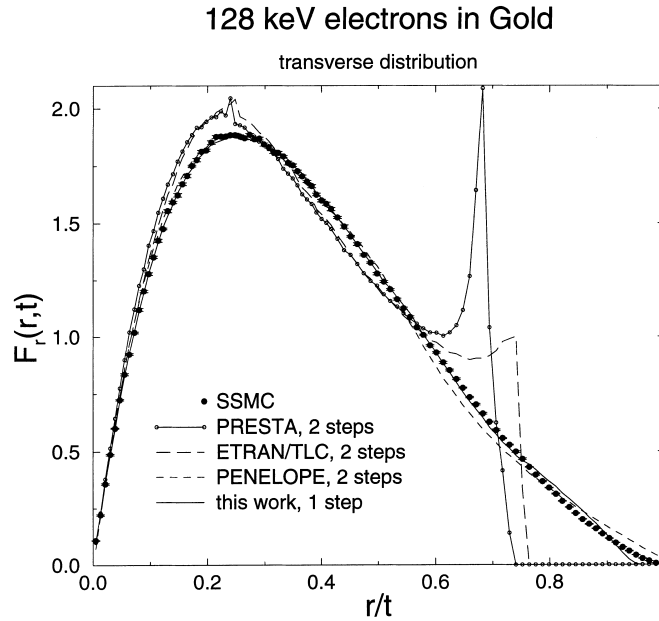
128 keV electrons in Gold

transverse distribution

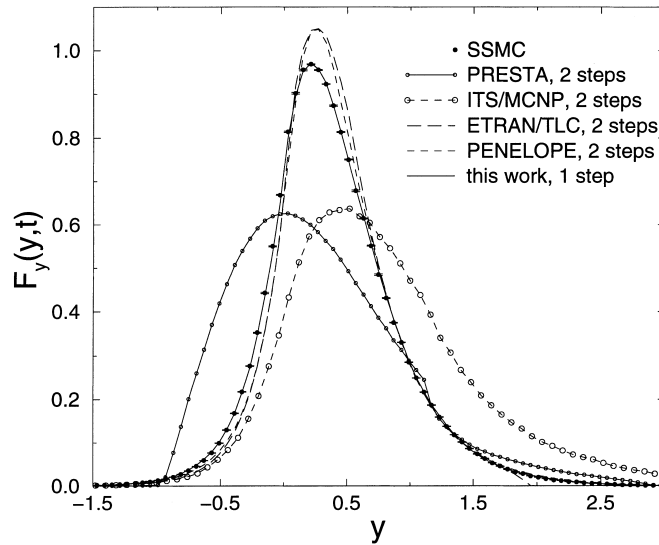Fig. 9. Radial distribution for the same situation as in Fig. 7.

Fig. 10. The distribution in the position-direction correlation variable y (see Eq. (81)) for the same situation as in Fig. 7.

6. Summary

In this paper we have studied available electron transport algorithms in terms of the moments of the spatial distribution and the average correlations between the electron's direction of motion and co-ordinates. This study is possible, for arbitrary moments and correlations, due to a generalization of Lewis' solution of the transport equation given in the Appendix.

Our analysis shows that electron transport algorithms currently in use have $O(\Delta s)$ or $O(\Delta s^2)$ truncation errors due to the condensed history technique. This observation is in agreement with Larsen's operator formalism study. The analysis of different ways of electron-step subdivisions indicates that there is no easy way of improving the convergence of the condensed history technique by simply mixing different transport and scattering strategies.

The new algorithm proposed in Section 4.4 is correct, for all moments studied, to $O(\Delta s^4)$ or better. Therefore, the truncation error of this algorithm after $1/\Delta s$ steps will be of the order of Δs^3, i.e. an order of magnitude better than the truncation error of previously proposed algorithms.

Finally, it is demonstrated in Section 5 that the new algorithm not only reproduces average quantities but approximates also very well the distributions in longitudinal and transverse direction resulting from the multiple scattering of the electrons.

Acknowledgements

Appendix A. Generalization of Lewis' solution of the electron transport problem

We will solve Eq. (1) under the boundary condition $f(\vec{x}, \vec{v}, 0) = \delta(\vec{x})\delta(v_x)\delta(v_y)\delta(1 - v_z)$, corresponding to a single particle, incident at the origin, and moving in z direction. Following Lewis [3] we expand the solution in normalized spherical harmonies in $\vec{v}$,

$$f(\vec{x}, \vec{v}, s) = \sum_{lm} f_{lm}(\vec{x}, s) Y_{lm}(\vec{v}), \qquad (A.1)$$

the cross section in Legendre polynomials P_l, and obtain from Eq. (1) and Eq. (A.1)

$$\frac{\partial f_{lm}}{\partial s} + \kappa_l f_{lm} = -\sum_{\lambda\mu} \vec{\nabla} f_{\lambda\mu} \cdot \vec{Q}_{lm}^{\lambda\mu}, \qquad (A.2)$$

where

$$\vec{Q}_{lm}^{\lambda\mu} = \int d\vec{v}\, Y_{lm}^*(\vec{v}) \vec{v} Y_{\lambda\mu}(\vec{v}) \qquad (A.3)$$

and κ_l given in Eq. (4). The boundary conditions to be satisfied by the f_{lm} are

$$f_{lm}(\vec{x}, 0) = \sqrt{\frac{2l+1}{4\pi}} \delta_{m0} \delta(\vec{x}). \qquad (A.4)$$

To solve Eq. (A.2), we multiply with $x^p z^q$ and integrate with respect to x, y and z. [5] If we define

---

[5] Because the problem is symmetric with respect to rotations around the z axis, it is sufficient to solve the equation for one of the transverse co-ordinates, x or y.

$$h_{l,m}^{p,q}(s) = \int dx\, dy\, dz\, x^p z^q f_{lm}(\vec{x}, s),\tag{A.5}$$

we obtain the following set of equations for the $h_{l,m}^{p,q}$

$$\left(\frac{\partial}{\partial s} + \kappa_l\right) h_{l,m}^{p,q} = \frac{p}{2}\left[A_m^l h_{l-1,m-1}^{p-1,q} + A_{m+1}^{l+1} h_{l+1,m+1}^{p-1,q} - A_{-m}^l h_{l-1,m+1}^{p-1,q} - A_{-m+1}^{l+1} h_{l+1,m-1}^{p-1,q}\right] + q\left[B_m^l h_{l-1,m}^{p,q-1} + B_m^{l+1} h_{l+1,m}^{p,q-1}\right]\tag{A.6}$$

with

$$A_m^l = \sqrt{\frac{(l+m)(l+m-1)}{4l^2-1}}, \qquad B_m^l = \sqrt{\frac{(l+m)(l-m)}{4l^2-1}}.\tag{A.7}$$

Eq. (A.6) can be solved in ascending order in p and q. For $p=0$, $h_{l,m}^{p,q} = 0$ unless $m=0$, and therefore Eq. (A.6) simplifies to Lewis' Eq. (25) for the longitudinal moments. For $q=0$ we obtain Lewis' Eq. (29) for the transverse moments. [6] We will give here two examples for mixed moments which can not be derived from Lewis' Eqs. (25) and (29). The lowest order such moments are of the form $\langle xzv_x^n v_z^m\rangle$ and can be calculated from $h_{l,m}^{1,1}$. We have $h_{l,m}^{1,1} = 0$ for $m^2 \neq 1$ and

$$h_{l,1}^{1,1} = -h_{l,-1}^{1,1} = \sqrt{\frac{l(l+1)}{16\pi(2l+1)}}\int_0^s ds' k_l(s-s')\int_0^{s'} ds''\left(\frac{k_{l-1}(s'-s'')}{2l-1}\left[2(l-1)k_{l-2}(s'') + k_l(s'')\right]\right.$$
$$\left. + \frac{k_{l+1}(s'-s'')}{2l+3}\left[k_l(s'') - 2(l+2)k_{l+2}(s'')\right]\right),\tag{A.8}$$

where

$$k_l(s) = \exp\left[-\int_0^s ds' \kappa_l(s')\right].\tag{A.9}$$

This gives, for instance,

$$\langle xzv_x\rangle = \frac{1}{15}\int_0^s ds' k_1(s-s')\int_0^{s'} ds''\left[5k_1(s'') + k_2(s'-s'')\left(k_1(s'') - 6k_3(s'')\right)\right].\tag{A.10}$$

By going to $p=2$ we find

$$\langle x^2 z\rangle = \frac{1}{15}\int_0^s ds' \int_0^{s'} ds'' k_1(s'-s'')\int_0^{s''} ds'''\left[10k_1(s''') + k_2(s''-s''')\left(8k_1(s''') - 18k_3(s''')\right)\right]\tag{A.11}$$

---

[6] Note that the subscript on the last term of the right hand side of Eq. (29) in Lewis' paper was wrong. His Eq. (29), from which the average correlation between longitudinal co-ordinate and direction of motion $\langle zv_z\rangle$ can be derived, contains also a typographic error. The correct formula reads

$$H_{l1} = \frac{k_l(s)}{\sqrt{4\pi(2l+1)}}\int_0^s ds' \frac{lk_{l-1}(s') + (l+1)k_{l+1}(s')}{k_l(s')},$$

where Lewis' function H_{l1} corresponds to our $h_{l,0}^{0,1}$. This leads to a missing factor 1/3 in Lewis' Eq. (28).

References

[1] M.J. Berger, Monte Carlo Calculation of the penetration and diffusion of fast charged particles, in: B. Alder, S. Fernbach, M. Rotenberg (Eds.), Methods in Comput. Phys., vol 1, Academic Press, New York, 1963, p. 135.

[2] E.W. Larsen, Ann. Nucl. Energy 19 (1992) 701.

[3] H.W. Lewis, Phys. Rev. 78 (1950) 526.

[4] S.A. Goudsmit, J.L. Saunderson, Phys. Rev. 57 (1940) 24.

[5] S.A. Goudsmit, J.L. Saunderson, Phys. Rev. 58 (1940) 36.

[6] M.J. Berger, R. Wang, Multiple-scattering angular deflections and energy-loss straggling, in: T. Jenkins, W. Nelson, A. Rindi, A. Nahum, D. Rogers (Eds.), Monte Carlo Transport of Electrons and Photons, Plenum Press, New York, 1989, p. 21.

[7] ICRU, Radiation dosimetry: Electrons with initial energies between 1 and 50 MeV, ICRU Report 21, ICRU, Washington DC, 1972.

[8] S.M. Seltzer, An overview of ETRAN Monte Carlo methods, in: T. Jenkins, W. Nelson, A. Rindi, A. Nahum, D. Rogers (Eds.), Monte Carlo Transport of Electrons and Photons, Plenum Press, New York, 1989, p. 153.

[9] S.M. Seltzer, Int'l J of Appl. Radiation and Isotopes 42 (1991) 917.

[10] D.W.O. Rogers, Nucl. Instr. and Meth. 227 (1984) 535.

[11] W.R. Nelson, H. Hirayama, D.W.O. Rogers, The EGS4 Code System, Report SLAC–265, Stanford Linear Accelerator Center, Stanford, California, 1985.

[12] A.F. Bielajew, Phys. Med. Biol. 35 (1990) 501.

[13] P. Andreo, Phys. Med. Biol. 36 (1991) 861.

[14] G.Z. Molière, Z. Naturforsch 2 (1947) 133.

[15] A.F. Bielajew, D.W.O. Rogers, PRESTA: The parameter reduced electron-step transport algorithm for electron Monte Carlo transport, National Research Council of Canada Report PIRS-0042, 1986.

[16] A.F. Bielajew, D.W.O. Rogers, Nucl. Instr. and Meth. B 18 (1987) 165.

[17] J.A. Halbleib, R.P. Kensek, T.A. Mehlhorn, G.D. Valdez, S.M. Seltzer, M.J. Berger, ITS Version 3.0: The Integrated TIGER Series of Coupled Electron/Photon Monte Carlo Transport Codes, Sandia report SAND91-1634, 1992.

[18] J. Briesmeister, MCNP – A general purpose Monte Carlo code for neutron and photon transport, Version 3A, Los Alamos National Laboratory Report LA-7396-M, Los Alamos, NM, 1986.

[19] MCNP – A general Monte Carlo N-particle transport code, in: J.F. Briesmeister (Ed.), Los Alamos National Laboratory Report LA-12625-M, Los Alamos, NM, 1993.

[20] A. Ferrari, P.R. Sala, R. Guaraldi, F. Padoani, Nucl. Instr. and Meth. B 71 (1992) 412.

[21] A. Fasso, A. Ferrari, J. Ranft, P.R. Sala, FLUKA: Present status and future developments, Proceedings of the Fourth Conference on Calorimetry in High Energy Physics, World Scientific, Singapore, 1994, p. 493.

[22] G.Z. Molière, Z. Naturforsch 3 (1948) 78.

[23] J.M. Fernández-Varea, R. Mayol, J. Baró, F. Salvat, Nucl. Instr. and Meth. B 73 (1993) 447.

[24] F. Salvat, J.M. Fernandez-Varea, J. Baro, J. Sempau, Penelope, an algorithm and computer code for Monte Carlo simulation of electron–photon showers, University of Barcelona preprint, 1996.

[25] I. Kawrakow, Nucl. Instr. and Meth. B 114 (1996) 307.

[26] I. Kawrakow, A.F. Bielajew, Nucl. Instr. and Meth. B 134 (1998) 325.